an Article from

Journal of Robotics and Mechatronics

7F Dai-ni Bunsei Bldg., 11-7, Toranomon 1-chome, Minato-ku, Tokyo 105, Japan
Tel: 03-508-0051 Fax: 03-592-0648

Paper:

Impedance Regulation in Human Movements During a Rotation Task

Koji Ito, Toshio Tsuji, and Minoru Sugino

Faculty of Engineering, Hiroshima University
1-4-1 Kagamiyama, Higashi-hiroshima-shi, Hiroshima 724, Japan
[Received May 18, 1991; accepted November 24, 1991]

In this paper, we discuss how the human subject controls the hand position and force depending upon the task objects and what roles the arm redundancy and muscle impedance regulation play in rotation. From the measurement of the hand force and arm posture in the execution of crank rotations, it was found that the subject made wrist joint impedance large and generated hand force in the both directions normal and tangential to the crank rotation. Impedance analysis demonstrated that the high impedance of the wrist joint, realized by simultaneous activities of the flexor and extensor muscles, provided for the posture of redundant arm without limiting the hand manipulatability. It was also shown that the hand force in the outer and normal directions contributed to an increase in the robustness of the hand manipulation against external disturbances.

Key-words: Arm redundancy, Impedance, Hand manipulation, Motor control, Force control

1. Introduction

The essence of movement control lies in the complex interactions between the environment and man's movements. In general, three types of variable are involved in the control of human movement: positional variables (displacement, velocity, acceleration), force-related variables (force, torque), and movement impedance variables (stiffness, viscosity, inertia). When rotating, pinching, or grasping an object in order to manipulate it with direct contact maintained between the fingers or hand(s) and the object, humans must control not only positional variables but also force variables according to constraints imposed by the object. Therefore, smooth manipulation requires that movement impedance connecting the two types of variables be properly set.

Mason et al.[1] proposed the hybrid control of the task space, in which a kinematic expression of constraints on the hands was defined. Salisbury[2] described the interactions between the hands and the surrounding environment by specifying a target stiffness and gave a control scheme to subserve the interactions. Hogan[3] proposed an impedance control, a generalized form of stiffness control, that related positional variables to force variables. It was intended to enable control by means of a software servo such that the impedance of hand manipulation from the environment would attain a specified value.

The human movement control system has a mechanism which regulates impedance. This resembles the mechanism that adjusts the variable visco-elasticity of muscles and parameters at the spinal cord level.[4] Dexterity of hand manipulation is attained with these regulating mechanisms and the kinematic mechanism of the muscle-skeletal system that effectively convey them to the hands. Hogan[5] used a mobility ellipsoid to analyze the movement impedance in the task space. Based on the analysis results, he identified important roles of the multi-joint muscles and the redundancy and posture of skeletal structure in regulating the impedance of hand manipulation.

Mussa Ivaldi et al.[6] experimentally determined the change in hand stiffness for various arm postures by providing forced displacement to the hands of the human subject and measuring their responses. Tsuji et al.[7,8] examined the movement impedance in the task spaces for muscle, joints, and task, as well as the methods of their transformation, in order to analyze the relationship between hand manipulatability and the transformation.

These studies all have one thing in common; from the perspective of tasks being under constraints imposed by the environment, they involved the theoretical analysis of how the general method of constructing impedance control and the redundant arm could be related to movement impedance.

Hand manipulation requires that the hand be provided with the appropriate force and impedance for the nature of the task, task objective, purpose, and features of the objects to be handled. However, it is not easy to describe the way force and impedance are set in a general form. Researchers have conducted basic studies including the expression of constraints on the hands[9] and the geometric/dynamic analysis of tasks performed with hands kept direct contact with the object.[10] In this sense, understanding how humans set impedance for attaining highly dexterous manipulation will help to theoretically analyze hand manipulation and to find the method for giving a robot manipulator instructions by which to control its force. However, with respect to human arm movement, most studies have dealt with kinematic analyses such as the control of finger position and trajectory[11,12] and letter-writing action.[13] Few have considered a manipulation task under constraints.[14]

Considering the background described above, the authors attempt to examine how humans regulate hand force and impedance depending on the type of task; here, a rotation task is used as an example. This is the first step of an in-depth study of impedance setting for hands. The authors will also analyze the roles of the arm redundancy and the impedance regulation at the muscle level in a rotation task. The paper is organized as follows: Section 2 defines motion impedance; Section 3 describes an experiment of a crank rotation task; Section 4 discusses the relationship among the

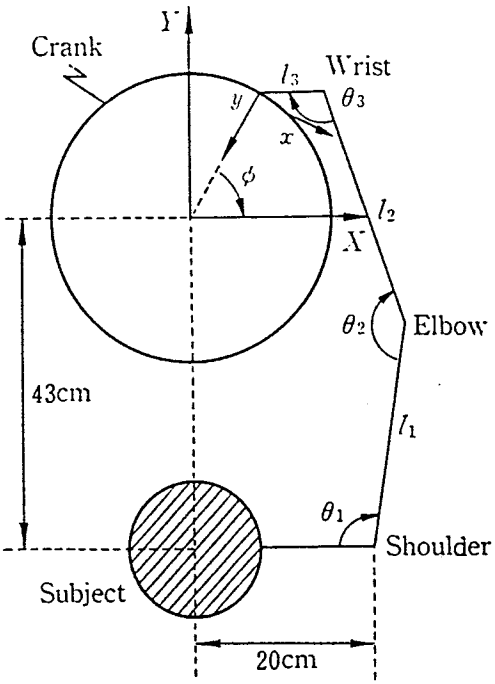

Fig. 1. Crank rotation task and coordinate systems

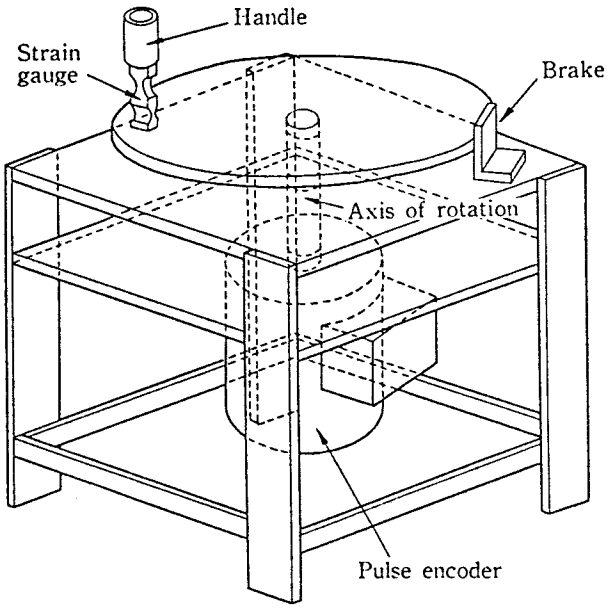

Fig. 2. Crank used in the experiment

rotation task, the arm redundancy, and the impedance regulation by using a dynamic model; and Section 5 verifies the analysis results given in Section 4 through the simulation of the rotation task.

2. Motion Impedance

Let the degree of freedom of the arm be n, a vector representing joint displacement be $\theta=(\theta_1, \theta_2, ..., \theta_n)^T$, and torque or force exerted on joints be $\tau=(\tau_1, \tau_2, ..., \tau_n)^T$. Also assuming that the task space is characterized by the m-degree of freedom, let the positional/posture vector be $X=(X_1, X_2, ..., X_m)^T$ and the force/moment vector be $F=(F_1, F_2, ..., F_m)^T$. If n>m, then the degree of freedom of the arm represents redundancy. In general, transformation from θ to X is non-linear and is given by

$$X = q(\theta) \quad \ldots\ldots\ldots\ldots\ldots\ldots (1)$$

Looking at infinitesimal displacement around the posture θ, we have

$$dX = J(\theta)\, d\theta \quad \ldots\ldots\ldots\ldots\ldots\ldots (2)$$

$J(\theta)=\partial q/\partial\theta \in R^{mxn}$ is called the Jacobian (Hereafter abbreviated to J).

Transformation from F to t is given by

$$\tau = J^T F \quad \ldots\ldots\ldots\ldots\ldots\ldots (3)$$

Thus, the expressions of motion in the task space and in the joint space can be combined with the Jacobian J.

Motion impedance, meaning mechanical impedance with respect to motion, transforms positional variables to force variables.

①stiffness: displacement →force $F=KdX$

②viscosity: velocity →force $F=Bd\dot{X}$

③inertia: acceleration →force $F=Md\ddot{X}$

The following linear model is often used as an impedance model[15]:

$$F = KdX + Bd\dot{X} + Md\ddot{X}$$

where dX is the deviation from equilibrium point.

Here the stiffness of the task space and joint space are given below.

$$\text{1) task space:} \quad F = K_e dX \quad \ldots\ldots\ldots\ldots (4)$$

$$\text{2) joint space:} \quad \tau = K_j d\theta \quad \ldots\ldots\ldots\ldots (5)$$

where $dX=X^e-X$, $d\theta=\theta^e-\theta$, and X^e and θ^e represent the respective equilibrium points. $K_e \in R^{mxm}$, and $K_j \in R^{nxn}$ are the stiffness matrices for the task space and joint space, respectively.

3. Experiment with Crank Rotation Task

3.1. Experimental Conditions

This experiment dealt with a task to rotate a crank in a horizontal plane. The subject stood with the center line of his body aligned with the center of the crank. He clasped the handle (15mm in radius) with his hand and rotated the crank. Two coordinate systems were used. One is a movable x-y coordinate system with the position of the handle as its origin, a straight line directed toward the center of the crank as the y-axis, and the tangent as x-axis. The other is the X-Y Cartesian coordinate system with the center of the crank as its origin (See **Fig.1**). **Figure 2** shows the construction of the crank used in this experiment. A pulse

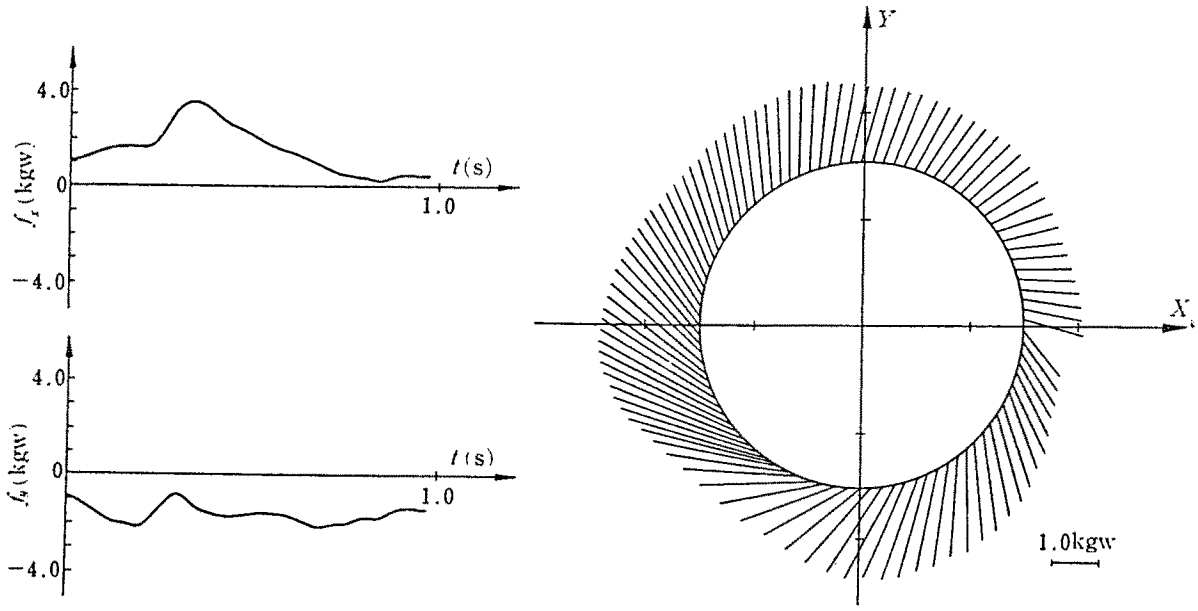

(a) Tangential force fx and normal force fy

(b) Hand force vectors

Fig. 3. Measurement results of hand forces (r=15cm, large friction)

encoder mounted on the axis of rotation of the crank measured the rotational angle (ϕ). Strain gauges mounted on the four faces of the lower portion of the handle measured the force vector f of the subject's hand which was expressed in the movable coordinate system. A goniometer fixed to the subject's wrist measured the wrist joint angle θ_3. Measurement was made at sampling interval of 10ms and data were entered into the computer at each interval. Experiment was performed on three radii of rotation; 15cm, 11.25cm, and 7.5cm. Tthe moment of inertia were 0.0534kgcm^2, 0.0495kgcm^2, and 0.0466kgcm^2, respectively. Low speeds ranged from 2 to 3rad/sec, and high speeds from 5 to 7rad/sec. In addition, a large Coulomb's frictional force, 0.107kgwm, and a small frictional force, 0.049kgwm, were used. Under these conditions, ten measurements were obtained. Two subjects were used for the experiment.

3.2. Experimental Results

For efficient crank rotation, it is necessary to control position and velocity of the crank by increasing tangential stiffness and viscosity while reducing normal stiffness. This allows the crank to exert its response because hard movements are constrained by the crank handle.[16] Because the rotation task was performed in a horizontal plane, the hand was provided with two degrees of freedom (for positional control and force control) and joints with three degrees of freedom, thus making the joint redundant.

1) Movements in the task space

Typical experimental results for a radius of rotation of 15cm and large friction are shown in **Fig.3**. Figure 3(a) indicates changes in the hand's tangential force (f_x) and in the normal force (f_y) toward the center of the crank as a function of time. Figure 3(b) contains the vectorial representation of Fig.3(a). For both figures, measurements were made with the crank being rotated clockwise at low speeds starting from ϕ=0°. As seen in the figures, the subject exerted a relatively constant tangential and normal forces. This trend is shared by the results for other combinations of the conditions. Fluctuation of f_x during rotation is primarily due to uneven frictional force.

2) Movements in the joint space

Figure 4 shows changes in arm posture for a radius of rotation of 7.5cm. Figure 4(a) shows the stick picture. Solid lines in Fig.4(b) represent changes in the joint angle with the top line corresponding to the shoulder joint, the middle line to the elbow joint, and the bottom line to the wrist joint. For all joints, the angle for a fully stretched joint is taken as 180°. The horizontal axis represents the crank rotation angle with its 0° position set at the x-axis. These figures indicate that the joint angles of the shoulder elbow joints underwent a smooth change from the stretched state to the bent state, closely following the rotation of the crank. However, the joint angle of the wrist joint showed only small change, maintaining an approximately 20° bend from the stretched state (180°) for the entire rotation process. In other words, the subject moved his wrist joint only slightly when rotating the crank. This tendency is also seen for the other experimental conditions.

Figure 5 shows the surface electromygrogram during rotation tasks measured concurrently with the measurement of the joint angle. The waveforms, from top to bottom, indicate activity of flexor of the shoulder joint angle, flexor of the shoulder joint (pectoralis major), extensor of shoulder joint (pectoralis major), extensor of the shoulder joint (infraspinatus), flexor of the elbow joint (biceps brachii), extensor of the elbow joint (triceps brachii), flexor of the wrist joint (flexor carpi radialis), and extensor of the wrist joint (extensor carpi ulnaris). It is seen from Fig.5 that although the flexor and extensor of the shoulder and elbow joints became alternately active, both muscles of the wrist joint were active for most of time. The concurrent state of activity indicates that the subject increased visco-elasticity around his wrist joint.[17] In other words, he actively locked

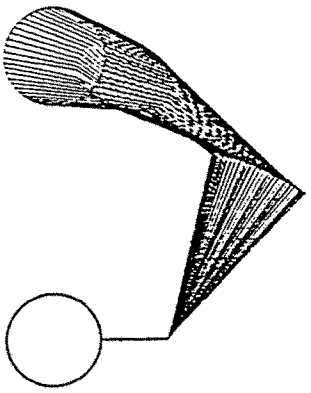

(a) Stick pictures

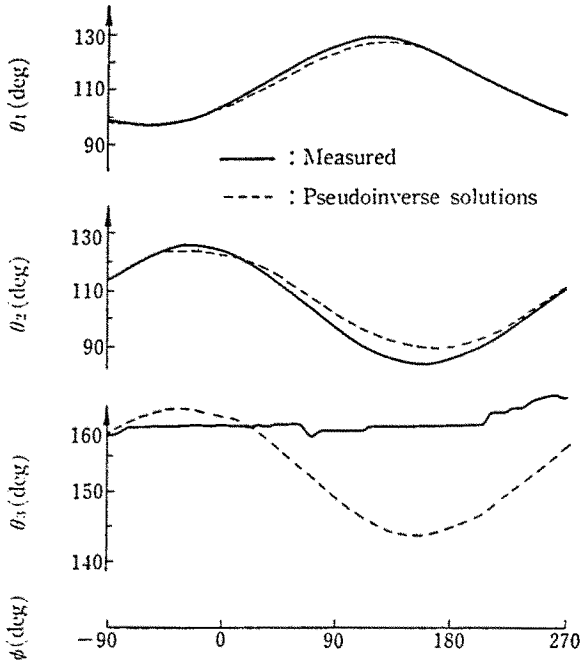

(b)θ_1: shoulder joint, θ_2: elbow joint, θ_3: wrist joint, ϕ: crank rotation angle

Fig. 4. Arm postures and joint angles

his wrist joint by increasing the visco-elasticity there. Based on these results, the authors presume that in rotation tasks such as that for a crank, humans do not coordinate the joint movements of the shoulder, elbow, and wrist but do tend to eliminate the redundancy by fixing the wrist joint.

4. Analysis of Rotation Task Model

4.1. Hand Manipulatability

If the wrist joint is locked, only the shoulder and elbow joints are free to move. This can cause considerable effects to hand manipulation. Therefore, the authors examined how joint torque affects hand manipulatability by focusing attention on hand joint stiffness.

The relationship between joint torque and hand displacement is calculated from Equations (2) and (5) and is expressed as follows, using the Jacobian matrix and stiffness

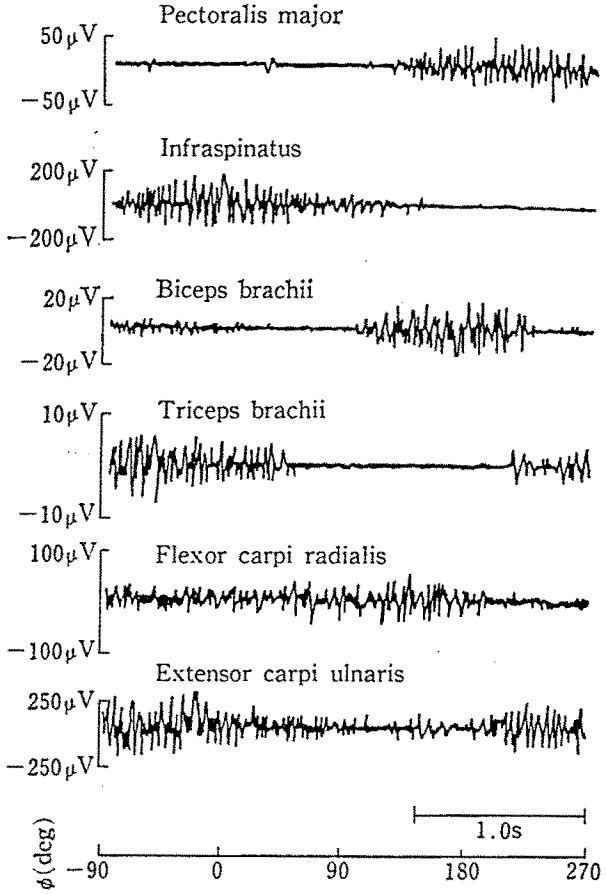

Fig. 5. Surface electromyogram (EMG) during rotation task

matrix K_j:

$$dX = JK_j^{-1}\tau \quad \ldots\ldots\ldots\ldots\ldots\ldots (6)$$

Now consider attainable displacement dX by using a constant joint torque $\|\tau\|^2=\tau_1^2+\tau_2^2+\cdots+\tau_n^2\leq 1$

The set of dX is given by an ellipsoid in the task space[8] as

$$dX^T[\,(JK_j^{-1})\,(JK_j^{-1})^T\,]^{-1}\,dX \quad 1 \quad \ldots\ldots\ldots (7)$$

The above equation can be regarded as an expression which describes, through the use of attainable displacement, the manipulatability of a hand whose position is changed by a constant joint torque.

Figure 6 shows hand manipulatability calculated from Equation (7) by using the subject's arm posture during crank rotation. Figure 6(a) is for relaxed shoulder, elbow, and wrist joints; (b) is for stiffened wrist joint, and (c) is for stiffened shoulder joint. Unlike relaxed joints (a), stiffened wrist joint (b) kept hand manipulatability almost constant. However, when the shoulder joint was stiffened, the ellipsoid was extremely small, indicating that only limited directions were allowed to the hand. This means that, with the wrist joint locked, joint torque is efficiently transmitted to the hands without impairing hand manipulatability. Thus, the human impedance regulating mechanism is highly efficient according to the type and requirements of the given task.

When the arm has freedom in redundant joint, the joint

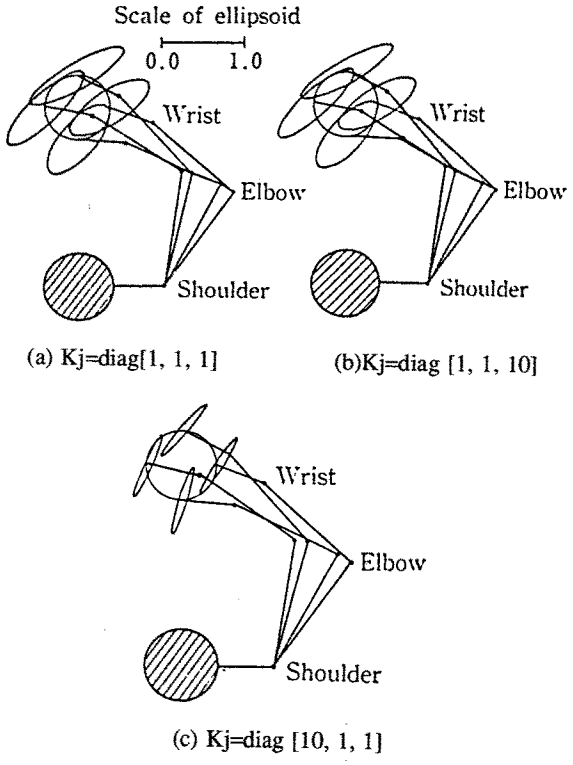

(a) Kj=diag[1, 1, 1] (b)Kj=diag [1, 1, 10]

(c) Kj=diag [10, 1, 1]

Fig. 6. Hand manipulatability

angle cannot be determined only from the hand position. To avoid this difficulty, inverse kinematic solutions have been proposed with a variety of evaluation criteria. They include pseudo-inverse matrices,[18] matrices for singularity low sensitivity resolved motion,[19] and joint torque optimization.[20] For example, one of the pseudo-inverse matrix solutions makes the sum of the squares of wrist joint displacement smallest. The dotted line in Fig.4 is the graphical representation of an inverse kinematic solution using pseudo-inverse matrices for this rotation task. While the wrist joint angle of the subject (the solid line) remained almost constant, the solution gives the same variation in wrist joint angle as in other joints. Inverse kinematic solutions based on other systems of evaluation criteria also kinematically define the posture of redundant arm. This approach separates them from regulating systems that rely on increased visco-elasticity of the wrist joint.

The authors previously described the method[7] to transform the hand stiffness onto the joint space. The solution obtained by this method is given in the form of a compliance (the inverse of stiffness that relates force to displacement) matrix:

$$C_j = J^+ C_e (J^T)^+ + \left[Z_1 - J^+ J Z_1 (J^+ J)^T\right] \quad \ldots\ldots (8)$$

where

C_e: compliance matrix for the task space
C_j: compliance matrix for the joint space
$J^+ = J^T (J J^T)^{-1}$: pseudo-inverse matrix

and $Z_1 \in R^{nxn}$ is an arbitrary matrix. C_j can be regulated by setting Z_1 while keeping C_e constant. Therefore, the redundant arm can select the proportion of the joint compliance to obtain a task space (hand) compliance (or stiffness). Thus, the selected proportion defines the posture of the redundant arm. In rotation tasks, humans make optimal use of his redundant arm to preset joint impedance, determine arm posture.

4.2. Robustness in Crank Rotation Tasks

This experiment revealed that the force vector of the hand was not always tangent but the outward direction.

Suppose that the crank is rotated clockwise under a constant rotational force, as shown in **Fig.7**, and that a subject standing at point A has set the normal force and the tangential force of F_r and F_x, respectively. With respect to rotational force components, the following relation holds:

$$M_e\ddot{\phi} + B_e\dot{\phi} + B_c \,\mathrm{sgn}\,(\dot{\phi}) = rF_x \quad \ldots\ldots\ldots (9)$$

where M_e, B_e, and B_c are inertia, viscosity, and Coulomb's friction for the crank, respectively, and r is the radius of the crank.

Assume that a disturbance has moved the crank by an angle of $\Delta\phi$ to the position P'. If F_r has been set outwardly normal, then its tangential component will face toward P. However, if F_r had been set inwardly normal, then its tangential component will face in the direction opposite to P.

The equation of motion for the rotational component after displacement is given by

$$M_e(\ddot{\phi} + \Delta\ddot{\phi}) + B_e(\dot{\phi} + \Delta\dot{\phi}) + B_c \,\mathrm{sgn}\,(\dot{\phi} + \Delta\dot{\phi})$$

$$= r(F_x \cos\Delta\phi - F_r \sin\Delta\phi) \quad \ldots\ldots\ldots\ldots (10)$$

ϕ and $\phi+\Delta\phi$ have the same sign. If Equation (9) remains true after displacement (due to the disturbance), Equation (10) can be rearranged as

$$M_e\Delta\ddot{\phi} + B_e\Delta\dot{\phi} + rF_r\Delta\phi = 0 \quad \ldots\ldots\ldots\ldots (11)$$

because $\Delta\phi$ is an infinitesimal. Equation (11) is
structurally stable if $F_r > 0$, or
structurally unstable if F_r

The dynamic characteristics of the crank in the vicinity of the equilibrium point structurally vary depending on the direction of the normal force vector.

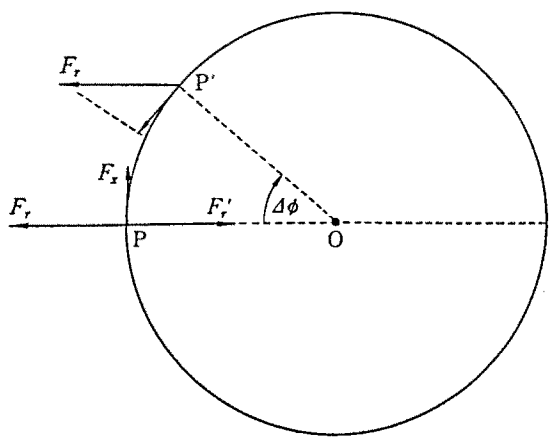

Fig. 7. Robustness of crank rotation

Therefore, the authors presume that when the angle of rotation for the crank deviates from the set position, the subject tries to exert an outward normal force in order to maintain structural stability, that is, to create a force which may restore the crank to the equilibrium point.

5. Simulation of Impedance Control

Through the aid of an impedance control system constructed on a hand manipulation coordinate system (3), use now consider a rotation task performed by a human subject (See Fig.8). Hand impedance that has preferable response to external force is expressed in the polar coordinate system as follows, with its origin set at the center of rotation of the crank.

$$M_d\ddot{\Phi} + B_d(\dot{\Phi} - \dot{\Phi}_d) + K_d(\Phi - \Phi_d) = -F_{int} \quad \cdots\cdots (12)$$

where Φ is defined as $\Phi=[\phi, r]^T$, ϕ is the rotational angle of the crank, and r is the distance from the center of rotation to the hand. M_d, B_d and K_d are the desired inertia, viscosity, and stiffness of the hand, respectively, in terms of polar coordinates. F_{int} is a force acting on the hand from the crank, $\Phi_d=[\phi_d, r_d]^T$ represents the equilibrium point of the hand.

The equation of arm motion expressed in polar coordinates is given by

$$M(\Phi)\ddot{\Phi} + h(\Phi,\dot{\Phi}) = F - F_{int} \quad \cdots\cdots (13)$$

where M(Φ) is the inertia matrix, h(Φ, $\dot{\Phi}$) is the centrifugal force/Coriolis effect, and F is the driving force of the hand. Gravity terms are omitted because the rotation task is performed in a horizontal plane.

Suppose that the following non-linear compensation allows for the centrifugal force/Coriolis effect

$$F = h(\Phi,\dot{\Phi}) + F_c \quad \cdots\cdots (14)$$

and that M_d=M(Φ), that is, the desired inertia is equal to the inertia of arm. Then, the functions surrounded by the dotted line in **Fig.8** can be made equal to the desired impedance, given by Equation (12), by applying a feedback operation as given by

$$F_c = B_d(\dot{\Phi}_d - \dot{\Phi}) + K_d(\Phi_d - \Phi) \quad \cdots\cdots (15)$$

Dividing Equation (15) into tangential (ϕ) and normal (r) components, we have

$$F_c = \begin{bmatrix} b_x & 0 \\ 0 & b_y \end{bmatrix}\begin{bmatrix} \dot{\phi}_\delta - \dot{\phi} \\ \dot{r}_d - \dot{r} \end{bmatrix} + \begin{bmatrix} k_x & 0 \\ 0 & k_y \end{bmatrix}\begin{bmatrix} \phi_\delta - \phi \\ r_d - r \end{bmatrix} \quad \cdots (16)$$

where hand impedance is expressed as diagonal matrices based on the assumption that there is no interference between components in the two directions.

Figure 9 shows the results of calculations performed under conditions that the crank is 15cm in radius, large stiffness is set at the hand in the direction tangential to the hand, and normal stiffness is zero. The appel method was used for the kinematic calculation of arm and crank movements. Simulation was conducted assuming the closed-link-structure which considers constraints on the hand.[21]

With impedance values preset at k_x=100, k_y=b_x=b_y=0, the authors defined instructions for movement as ϕd =ϕ+0.02(rad), and $r_d = r$. In addition, the authors expressed the initial posture of the hand with measurements obtained in the experiment ($\theta_1(0)$=2.39rad, $\theta_2(0)$=1.69rad, $\theta_3(0)$=2.64rad). Figure 9(a) indicates the changes in tangential force and normal force of the hand with time, and Fig.9(b) indicates the change of arm posture and of force vector of the hand. From these figures it is seen that the force vector was set nearly in the tangential direction. A large variation at around t=1.4 second represents a singular point where the wrist was fully stretched. Also the wrist joint was in forced posture due to the arm redundancy. This is because the control system employed in this simulation does not give a target angle for the wrist joint but defines only positional feedback of the hand in the task space. This problem can only be solved by forming a control system at the joint level from inverse kinematic solutions taking the movable zone into account.

However, a wrist joint with as large an impedance as a human's is considered here. To simulate this, the authors used impedance control given by Equation(16) in addition to a high-gain local feedback on the wrist joint given by

$$\tau_{wrist} = K_{wrist}(\theta_3(0) - \theta_3(t)) - B_{wrist}\dot{\theta}_3(t) \quad \cdots (17)$$

The results of the simulation are presented in **Fig.10**. Because redundancy was eliminated, a control of the arm in natural posture was possible as long as initial posture was properly chosen.

Normal stiffness was defined as zero in this simulation, therefore, the force vector was in the tangential direction except for a slight effect of mutual interference between the two directions (tangent and normal). The outward force vector, like that for humans, can be obtained by providing impedance control on the task coordinates, as given by the Equation(16), with proper normal impedance and, by providing the equilibrium point (r_d) with a setting greater than the actual crank radius. The results of this calculation are shown in **Fig.11**. It is noted that if the equilibrium point is set to a value smaller than the actual radius, then an inward force vector will result. Thus, impedance setting and the magnitude of the radius of rotation as an imaginary target determine the direction of force vector.

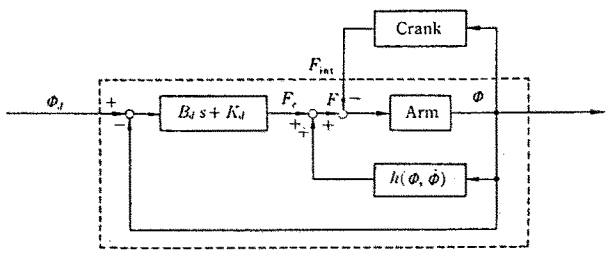

Fig. 8. Block diagram of impedance control system

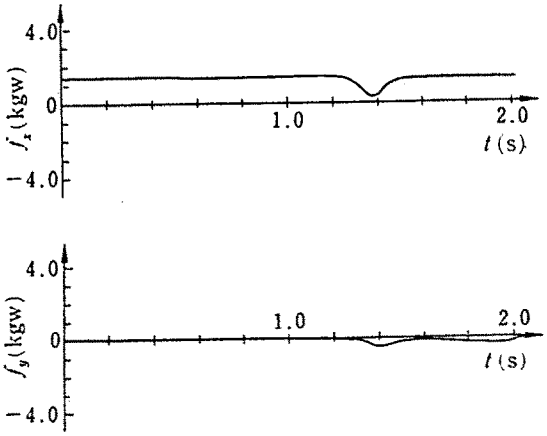

(a) Tangential force f_x and normal force f_y.

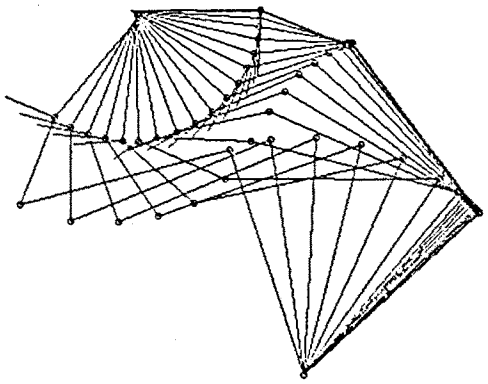

(b) Stick pictures

Fig. 9. Simulation I: stiffness control in hand coordinates

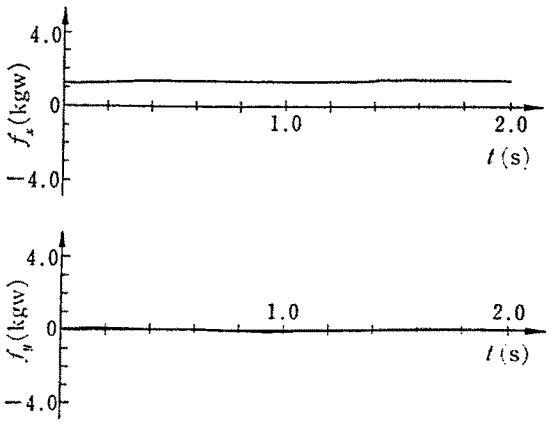

(a) Tangential force f_x and normal force f_y

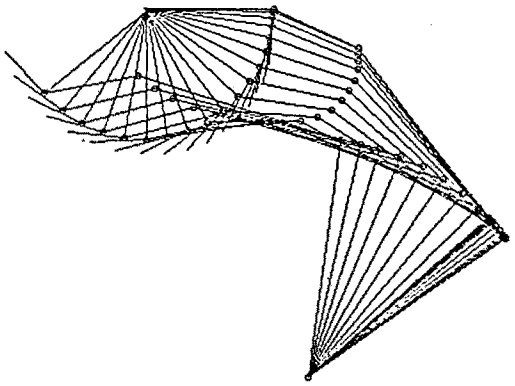

(b) Stick pictures

Fig. 10. Simulation II: with stiff wrist joint [K_{wrist}=10, B_{wrist}=0.1]

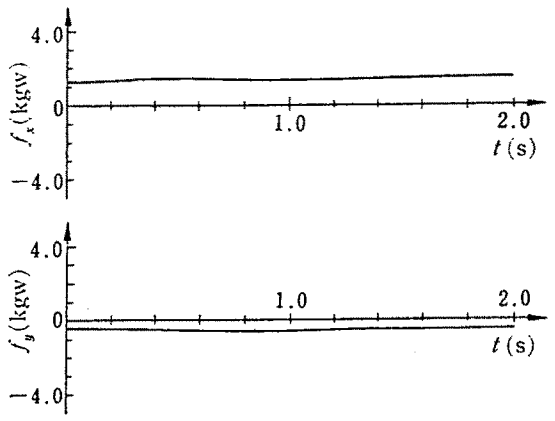

(a) Tangential force f_x and normal force f_y

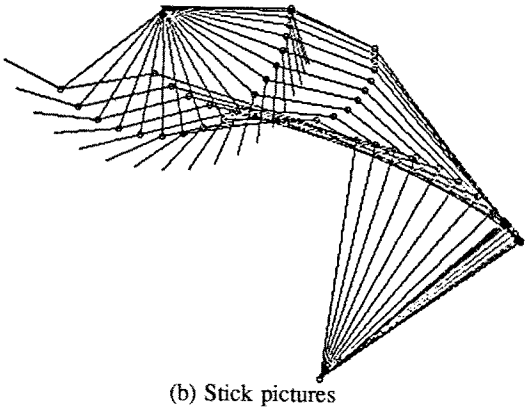

(b) Stick pictures

Fig. 11. Simulation III: generation of force vectors in the direction normal to the crank rotation [k_y=50, r_d=r+0.1]

6. Conclusion

This paper presented an analysis of human hand force during a crank rotation task in an attempt to provide an approach to methods of setting hand impedance in accordance with the nature of the given task. The analysis has revealed that humans dexterously adjust hand force and hand impedance based on the nature of the task. Also, optimal use of impedance regulating mechanism featured by concurrent activities of the flexor and extensor of the muscles is achieved to set impedance at the wrist joint for the given task. This process of control defines the posture of redundant arm while allowing manipulatability of the hand to be properly maintained. It also provides the hand with robustness against external disturbances. These findings may be applied to other types of rotation tasks such as opening and closing doors.

The authors feel it is necessary to further study the optimum allocation of motion impedance to each joint in the redundant arm as well as to find a general method of impedance setting appropriate for the objects and the nature of task.

This study was conducted in part through research subsidies of the Ministry of Education (62460142, 63750415). The authors are deeply thankful to those concerned.

References:

1) M.T. Mason, "Compliance and Force Control for Computer-Controlled Manipulators," IEEE Trans. Systems, Man, and Cybernetics, SMC-11-6, pp.418-432 (1981).
2) J.K. Salisbury, "Active Stiffness Control of a Manipulator in Cartesian Coordinates," Proc. of IEEE Conf. on Decision and Control, pp.95-100 (1980).
3) N. Hogan, "Impedance Control: An Approach to Manipulation"; Part I, II, III, Trans. the ASME. J. of Dynamic Systems, Measurement and Control, 107-1, pp.1-22 (1985).
4) K. Ito, "Muscle Motor Control Mechanism, Measurement and Control," 25-2, pp.131-135 (1986).
5) N. Hogan, "The Mechanics of Multi-Joint Posture and Movement Control," Biological Crybern., 52, pp.315-331 (1985).
6) F.A. Mussa Ivaldi, N. Hogan, and E. Bizzi, "Neural, Mechanical, and Geometric Factors Subserving Arm Posture in Humans," J. Neuro Science, 5, pp.2737-2743 (1985).
7) Tsuji et al., "Impedance Transformation in Multi-degree of Freedom Movement of Redundant Arm," Trans. the Society of Electrical Engineers, 108C-7, pp.471-477 (1988).
8) Tsuji et al., "Impedance Regulation Mechanism of Muscle Motor Control System and Hand Manupilatability," Trans., the Society of Instrument and Control Engineers 24-4, pp.385-392 (1988).
9) T. Yoshikawa, "Dynamic Hybrid Control of the Position and Force of Robot Arm the Description of Constraints on the Hand and the Calculation of Driving Joint Force," Journal of Japan Robotics Society, 3-6, pp.531-537 (1985).
10) Suehiro and Takase, "Expressions of Contact Movements, Its Control, and Their Application to Assembly Work," Journal of Japan Robotics Society, 6-6, pp.499-506 (1988).
11) W. Abend, E. Bizzi, and P. Morasso, "Human Arm Trajectory Formation," Brain, 105, pp.331-348 (1982).
12) Y. Uno, "Formation of Movement Trajectory and Learning System," Computrol, 24, pp.29-37 (1988).
13) Taguchi and Fujii, "Expression of Brain Functions for the Movement Control of Letter Writing," Journal of Society of Electronic and Communication Engineers, J70-D-3, pp.640-649, (1986).
14) Asada and Asari, "Identification of Tool Holding Impedance by Means of the Measurement of Movements of Skilled Workers, and the Method of Giving a Robot Directions for Work Procedures," Trans. the Society of Instrument and Control Engieners, 24-12, pp.1292-1298 (1988).
15) H. Kazerooni, T.B. Sheridan, et al., "Robust Compliant Motion for Manipulators," Part I and II, IEEE J. Robotics and Automation, RA-2, pp.83-105 (1986).
16) Yokoi, Kaneko, Miyajima, Ohno, and Tanie, "Direct Compliance Control by a Three Degrees of Freedom Manipulator," 2nd Report on Application to Rotation Tasks, Proc. of 4th Meeting by Japan Robotics Society, pp.447-448 (1986).
17) Ito and Tsuji, "Bi-linear Characteristics of Human Muscle-Skeltal-System and Their Application to the Control of Artificial Limbs," Trans. the Society of Electrical Engineers, 105C-10, pp.201-208 (1985).
18) D.E. Whitney, "Resolved Motion Rate Control of Manipulators and Human Prostheses," IEEE Trans. Man-Machine Systems, MMS-10-2, pp.47-53 (1969).
19) Y. Nakamura and H. Hanafusa, "Inverse Kinematic Solutions with Singularity Robustness for Robot Manipulator Control," Trans. the ASME., J. of Dynamic Systems, Measurement and Control, 108, pp.163-171 (1986).
20) J.M. Hollerbach, "Redundancy Resolution of Manipulators Through Torque Optimization," IEEE J. Automation and Robotics, Ra-3, pp.308-316 (1987).
21) Yokoyama, Ito, and Tsuji, "Analysis of Constrained Movements Through the Use of a Human Movements Analyzing System," Technical Report, the Society of Electronic Information and Communications Engineers, MBE89-45, pp.29-36, (1989).